Quarterly Report

Project Title:
Development of a Self-Sustained Wireless Integrated Structural Health Monitoring System for Highway Bridges

Cooperative Agreement # RITARS11HUMD

Third Quarterly Progress Report

Period:
January 15, 2012 through April 14, 2012

Submitted by:
The Research Team – University of Maryland with North Carolina State University and URS

Submitted to:
Mr. Caesar Singh, Program Manager, US DOT

Date: April 28, 2012

Table of Contents

EXECUTIVE SUMMARY

I — TECHNICAL STATUS

Accomplishments by Milestone

1.1. General

- Submitted presentation slides to The Sensing Technologies TRB Subcommittee (Task 6 and Deliverable 12)
- Interviewed Drs. Fu, Zhang and Yuan by ASCE Civil Engineering Magazine Senior Editor Robert Reid and article appeared on the April 2012 issue. (Task 6 and Deliverable 12) (http://www.civilengineering-digital.com/civilengineering/201204?pg=40&search_term=chung fu#pg40)
- Updated Project web site (http://www.ncrst.umd.edu/) (Task 1 and Deliverable 2)
- Delivered Second quarterly financial and technical reports (Task 6 and Deliverable 11)
- Conducted meeting with NCDOT by Drs. Yuan (NCST) and Fu & Zhou (UMD and URS, traveled from MD) at 11:00AM on the February 3, 2012. The meeting was hosted by the State Bridge Design Engineer Chief Greg Perfetti. NCDOT Structure Design Unit. Daniel Muller, PE, NCDOT Structures Management Unit, was designated as the contact person for selecting testing bridges and its logistics.
- Conducted meetings with MDSHA at 10:00AM on January 6, 2012 on selecting the second bridge for pilot test site. (The baseline, the first one tested, bridge in Maryland is US 1 bridge over Paint Branch.) Br0305602, IS83 SBR over Thornton Mill Rd is our first candidate pilot bridge. Field trip was made on the February 24, 2012

and frequency measurements and preliminary analysis were conducted on detecting possible fatigue activity.

- Better candidate, MD Bridge No. 1504200 I-270 over Middlebrook Road, was recommended by Dr. Zhou of URS to the UMD. Preliminary report was made by Dr. Zhou to the State of Maryland and the plan was approved. Field test was scheduled to be on March 19-21, 2012 during the University spring break.
- The proposed work plan is shown below as Milestones/Deliverables. Dark Shading indicates Deliverable items and Tasks in which the Research Team has been engaged over the past quarters. Lighter shading indicates anticipated duration for Deliverables by quarter.

Deliverables	Action	Quarter No.									
		1	2	3	4	5	6	7	8	9	10
1	Form TAC and conduct kick-off meeting. Determine baseline field test procedure (Task 1)										
2	Establish and update project web site (Tasks 1 & 6)										
3	Conduct baseline field test and finite element analysis on pre-selected bridges (Task 1)										
4	Design, fabricate and characterize AE sensor and measure the performance (Task 2)										
5	Develop and evaluate T-R method for passive damage interrogation (Task 3)										
6	Develop and experimentally evaluate wireless smart sensor and hybrid-mode energy harvester (Task 4)										
7	Implement passive damage interrogation T-R algorithm in the wireless smart sensor on bridges (Task 4)										
8	Integrate and validate AE sensors with wireless smart sensor and hybrid-mode energy harvester (Task 5)										
9	Develop and conduct field implementation/validation of commercial-ready ISHM system with remote sensing capability (Task 5)										
10	Recommend strategy to incorporate remote sensing and prognosis into BMS (Task 5)										
11	Prepare and submit quarterly status and progress reports and final project report (Task 6)										
12	Submit paper to conference presentations and publication to TRB meeting or other conferences (Task 6)										

1.2. PXI System by National Instrument (http://www.ni.com/pxi/)

- Converted UniMeasure, Inc. potentiometer's electrical to look like a full bridge in order to acquire displacement data with our PXI-4330 Bridge Input Module.
  - Calibrated Labview to read the potentiometers and convert analog bridge measurements (V/V) into displacement (inches).
- Formatted Labview to correctly implement strain gage factors with their corresponding strain transducers from Bridge Diagnostics, Inc (BDI)
- Configured Labview to read and utilize fatigue virtual instruments
  - Instruments utilize a "Stress Life" method of fatigue analysis for high cycle fatigue testing
    - S-N curve characteristics
    - Rainflow Cycle Counting
    - Power Spectral Density (PSD) and Probability Density Function (PDF)
    - Palmgren-Miner Rule for total damage estimation

1.3 Pilot Bridge Testing

- Performed preliminary pilot bridge testing - Br0305602, IS83 SBR over Thornton Mill Rd was visited on Feb. 24 first. Better candidate on MD Bridge No. 1504200 I-270 over Middlebrook Road was later selected and complete pilot testing was performed on March 19-21, 2012, using AE, accelerometer, deflection and strain sensors for bridge information collection. Maximum stress range measured above the diaphragm on girder web in the longitudinal direction is 1.6 ksi due to regular traffic. Stress range records were collected, which will be used as a reference for future testing. (Task 2 and Deliverables 4 & 9)
- Conducted validation of the first pilot bridge field test – FEM model of this pilot bridge was established. Appendix A shows the frequency test of Br0305602, IS83 SBR over Thornton Mill Rd. (Task 2 and Deliverables 4 & 9)
- Conducted full test of the second pilot bridge field test – Full test was conducted and its FEM analyses of this pilot bridges were conducted. Appendix B shows the complete report of MD Bridge No. 1504200. (Task 2 and Deliverables 4 & 9)
- Analyzed and organized detailed structural information of the Swing Bridge at Beaufort County by the NCST team and report on the preliminary investigation of this bridge is shown in Appendix C I-270 over Middlebrook Road. (Task 3 and Deliverable 5 & Task 4 and Deliverable 6)

1.4 AE Sensor

- Conducted pilot test bridges in Maryland: Wireless sensors were used on the pilot test bridge (I83 Bridge near Hunt Valley, Maryland, and I270 Bridge near Germantown, Maryland) to measure its vibration frequency. The measured information was used for calibrating finite element models for the two steel I-girder bridges. On the I270 Bridge, piezo paint AE sensors were installed to characterize its performance in real operating environment. Also, new types of noncontact displacement sensors including laser distance sensor and ultrasonic distance sensor were used to measure bridge deflection.

- Designing and testing AE sensor in the lab - Major work conducted in the third quarter includes (1) a new batch of flexible piezoelectric paint was fabricated on March 8, 2012. (2) New design of piezo paint based acoustic emission (AE) sensors were fabricated by an external flexible circuit manufacturer – Tramont (order received in February) and sensor performance was examined in lab in March and April 2012; (3) Fatigue test frame and specimens (including six test steel tube with welded end plate specimens and load frames) were fabricated and delivered in early February. This test frame and specimens will be used for conducting lab characterization test of low-profile piezoelectric paint based AE sensor in the summer of 2012; (4) a new frequency shift based crack source location algorithm is proposed and verified through lab calibration experiments (see Figure 1 below). This near-field AE monitoring strategy is being refined for low-profile piezoelectric paint based AE sensor and has the advantage of improved representation of crack source information. and (5) Fatigue test of a portable setup to simulate fatigue crack propagation (see Figure 2 below) was conducted in January 2012. The setup consists of a steel base plate, two steel bars welded to the base plate and proper weight to simulate the bridge vibration frequency (around 3.4 Hz). Piezoelectric paint sensors have been installed on base plate to monitor any AE signal caused by fatigue crack initiation and propagation; (6) A Labview-based virtual instrument software for data acquisition of AE data was developed but still need improvement including the new frequency shift feature for crack source location.

Figure 1. Calibration setup for piezo paint AE sensor

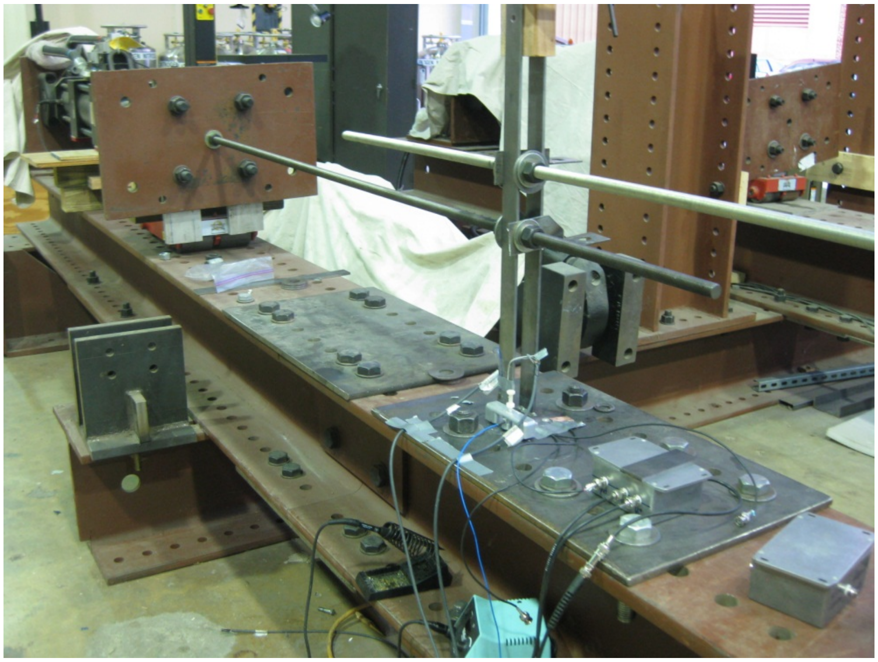

Figure 2. Fatigue test setup for portable fatigue simulation rig

1.5 T-R Method, Energy Harvesting and Smart Sensor

Accomplishments of these tasks are detailed in Appendix C and summarized here:

- Analyzed and organized detailed structural information of the Swing Bridge at Beaufort County (Task 3 and Deliverable 5 & Task 4 and Deliverable 6)
- Developing signal and data transmission paths (Gateway Protocol). (Task 4 and Deliverable 6)
- Designing and manufacturing wind turbine energy harvester-based on the experimental result of the miniature wind turbine (MWT). (Task 4 and Deliverable 6)
- Developing and evaluating a new Buck-Boost Converter. (Task 4 and Deliverable 6)
- Developed a new wireless accelerometer board. (Task 4 and Deliverable 6)
- Enhanced a new wireless sensor based on the prototype wireless intelligent sensor platform developed at the NC State. (Task 4 and Deliverable 6)
- Enhanced and evaluated physics-based model (Task 3 and Deliverable 5 & Task 4 and Deliverable 6)
- Enhanced and evaluated wind turbine energy harvester (Task 4 and Deliverable 6)

1.6 Future Plans

Pilot Bridge Testing -

- Continue evaluating and validating results from the 2nd pilot testing bridge (MD Bridge No. 1504200 I-270 over Middlebrook Road)
- Long-term monitoring using AE sensors on the pilot test bridge in Maryland
- Field testing T-R method, energy harvesting and smart sensors on the pilot test bridge in NC
- Simulating traffic through FEM models for all pilot test bridges in Maryland and NC

- Validating test data with FEM results

AE Sensor -

- Conducted baseline test bridges in Maryland and NC: In the next quarter, new design of piezo paint AE sensors (for optimal crack source location based on frequency shift) will be installed and tested for its performance on I270 Bridge near Germantown, Maryland. A longer monitoring period (3 to 5 days) will be used to monitor the fatigue crack induced acoustic emission signals and possible fatigue crack growth during the monitoring period. Integrating wireless transmitter with piezo paint AE sensor is planned during the field test.
- Continue testing AE sensor in the lab - piezo paint AE sensor with new pattern to maximize frequency shift caused by fatigue crack growth will be tested in the steel welded tube specimens in lab. The next quarter will involve characterizing these AE sensors with integrated wireless sensing feature.
- Fabrication of higher sensitivity piezo paint is planned in the next quarter after a vacuum chamber is assembled in lab.

T-R Method, Energy Harvesting and Smart Sensor -

- Finishing the signal and data transmission programs before the accelerometers installed.
- Manufacturing the Buck-Boost Converter. The miniature wind turbine system to be capable of converting wind energy into electrical energy and storing it in rechargeable battery will be finished.
- Finish the PCB design of the new wireless accelerometer board and send the design to PCB factory, write programs to debug it.
- Order the circuit components and solder the new wireless accelerometer boards and solar energy panel and Lithium battery.
- Assemble the wireless accelerometer sensors.

II — BUSINESS STATUS

- Hours/Effort Expended – PI Dr. Fu worked one month paid by his cost sharing account for 167 man-hours. Three (3) UM and two (2) NCSU graduate assistants worked three months half-time (20 hours), the quarterly accounting deadline, for a total of 1,470 man-hours (one NCSU assistant is partially cost-shared by their University.)
- Hours/Effort spent by the MD & NC States for in-kind cost share are not counted for here.
- Funds Expended and Cost Share –
  - Listed and invoiced in this Quarterly Federal Financial Report (period ending on March 31, 2012): Federal share of expenditure requested for this quarter $80,318.66 [Federal share total $214,390.05; Recipient share of expenditure (cost share) $18,388.88; Cumulative Total $232,779.93]

- Spending not included in this last Quarterly Federal Financial Report but included in this report: NCSU invoice to 4/10/2012 $18,156.20 (total cost share today $14,406.27), in-kind cost sharing contribution by MDSHA on equipment, personnel, consultation, road-side assistance on the March 26-28 bridge test, and in-kind cost sharing contribution by NCDOT on the search for candidate and field trips.
- Listed and invoiced in this Quarterly Federal Financial Report (period ending on March 21, 2012): (the following with matching marked are from the $50K match of Dr. Y. Zhang's startup account)
    1. Honda electrical generator (for field test), $2200 + shipping
    2. Thrifty Iron Works, Inc., fatigue load frames, $8100.00 (matching)
    3. SAP2000 and Bridge Module software, $500.00 (matching)
    4. Laser distance sensors, $1,926.00 (matching)

Appendix A – Field Trip Report on Br0305602, IS83 SBR over Thornton Mill Rd

Appendix B – UMD Report for MD Bridge No. 1504200 I-270 over Middlebrook Road

Appendix C - NCST Report for NC Structure No. 060025 Swing Bridge at Beaufort County

Appendix A – Field Trip Report on Br0305602, IS83 SBR over Thornton Mill Rd

February 24, 2012 Field Test on I83 Thorton Mill Bridge (Southbound) near Hunt Valley, Maryland

Bridge Type: Steel I-girder Bridge

Figure 1. View of the bridge

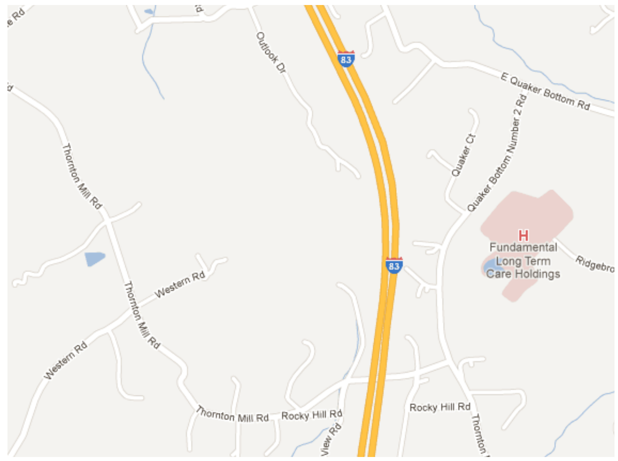

Figure 2. Bridge location (red circle)

Figure 3. Fatigue crack on girder web location (at the weld intersection of diaphragm and web plate)

Figure 4. Wireless sensor (measuring acceleration) at south side (about 10 ft from abutment) of the bridge

Figure 5. Wireless sensor (measuring acceleration) at north side (about 7 ft from abutment) of the bridge

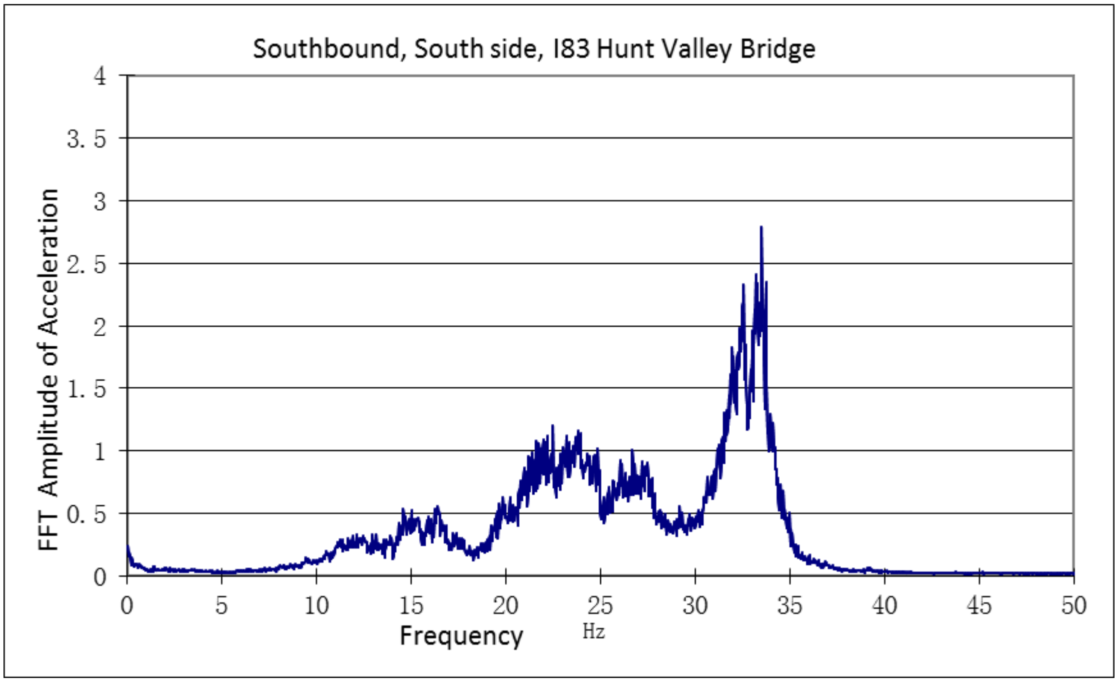

Figure 6. FFT amplitude of measured acceleration at southside of the bridge (average of 10 records, each record has duration of 30 seconds, and sampling rate of 100 Hz)

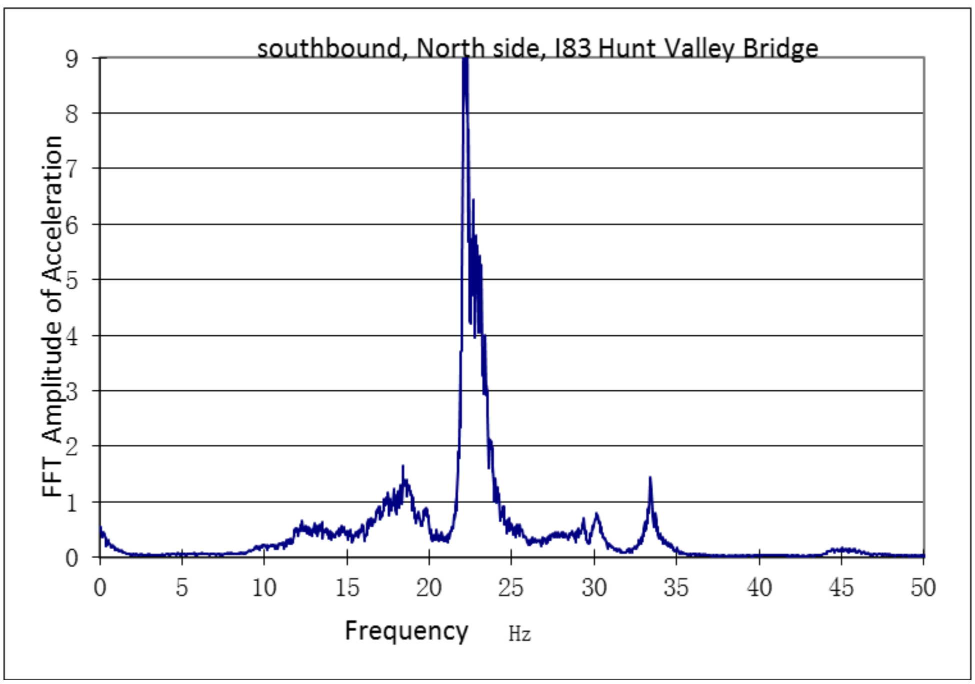

Figure 7. FFT amplitude of measured acceleration at north side of the bridge (average of 10 records, each record has duration of 30 seconds, and sampling rate of 100 Hz)

Appendix B – Field Test Report for Bridge No. 1504200 I-270 over Middlebrook Road

By

Dr. Chung C. Fu, PE, and Dr. Yunfeng Zhang

Field test dates: March 19 to 21, 2012
Bridge Type: Single-span composite steel I-girder bridge (span length = 140 ft.; Figure 1)
Location: I-270 Middlebrook Bridge (Southbound) near Germantown, Maryland (Figure 2)
Participants:

UMD Dr. Fu's group: Dr. Chung C. Fu; Graduate Students: Tim Saad and Time Brinner (BDI strain transducer and Cable-Extension Transducer, or called string pot)

UMD Dr. Zhang's group: Dr. Yunfeng Zhang; Graduate Students: Changjiang Zhou (AE sensor), Linjia Bai (wireless sensor), Zhen Li (laser distance sensor), and Feng Shi (ultrasonic distance sensor)

URS Dr. Ed Y. Zhou (part time)

Figure 1. View of the bridge

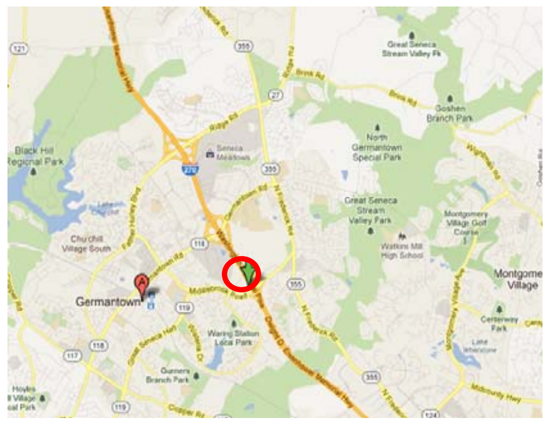

Figure 2. Bridge location (red circle, latitude=39.175296, longitude= -77.247046)

PHASE I – INSTRUMENTATION PLAN

The main data acquisition (DAQ) systems used in this test are:

a. PXI-based data acquisition system by National Instruments which was used for data collection by BDI strain transducers, string pots and AE sensors
b. Multi-channel data acquisition equipment CR5000 manufactured by Campbell Scientific, Inc. for extra BDI strain transducer

Types of sensors used in this project are: 1. piezoelectric paint AE sensors; 2. wireless accelerometers; 3. laser sensor; 4. ultrasonic distance sensors; 5. BDI strain transducers; and 6. String pots.
Instrumentation plan is shown in Figure 3 – Crack locations and sensor placement on the framing plan. Also shown are Figures 4-7 for cracks on Girders 3 & 4 and their respective sensor locations.

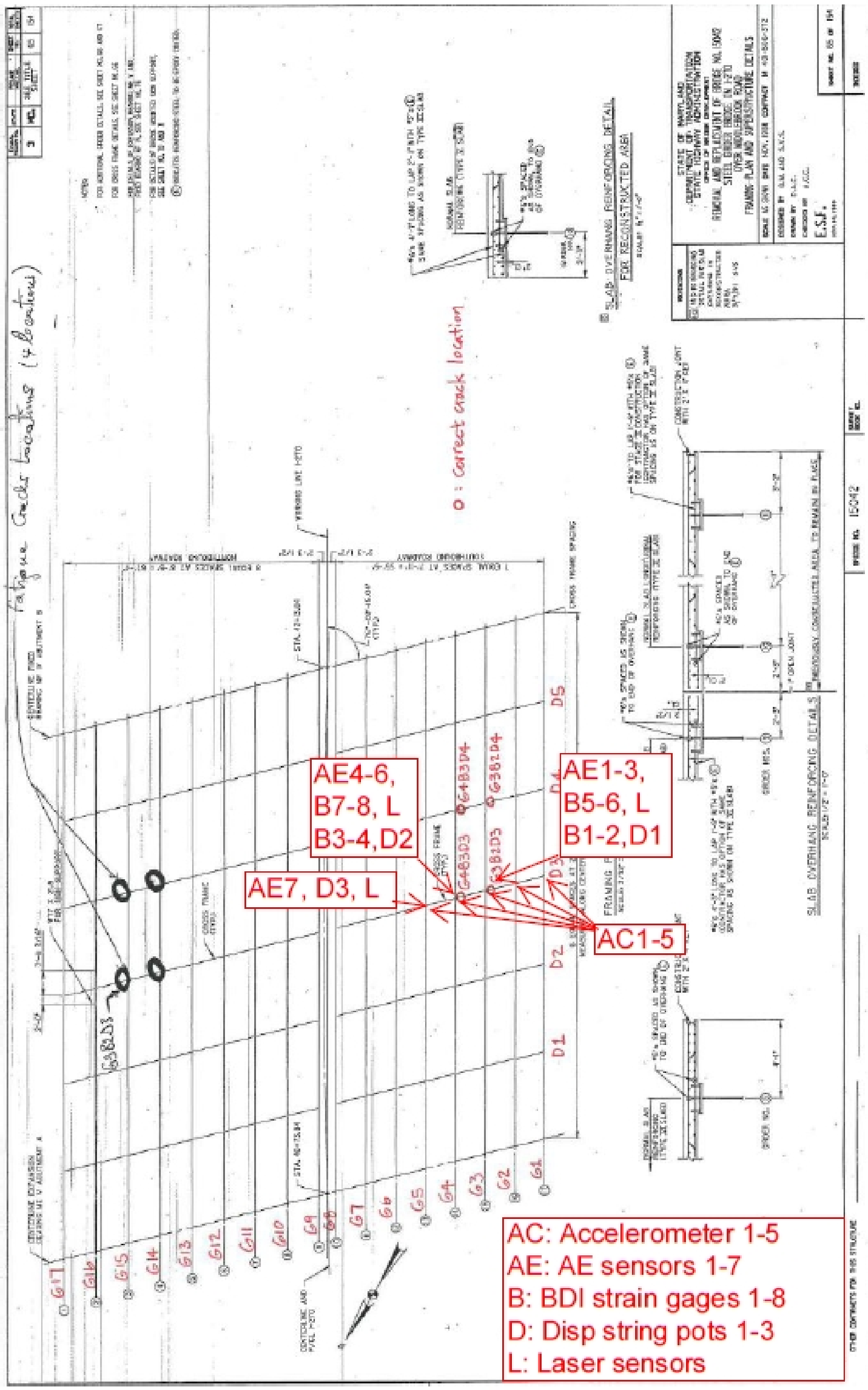

Figure 3 – Crack locations and sensor placement on the framing plan

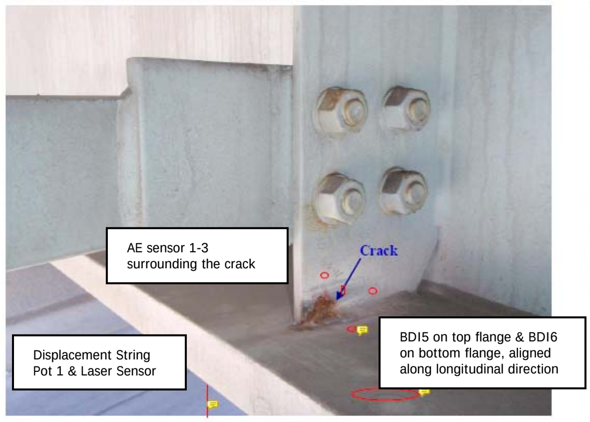

Figure 4. Crack at G3B2D3 (Girder 3 Bay 2 Diaphragm 3) and sensor

Figure 5. No Sign of Cracking at G3B3D3 (Girder 3 Bay 3 Diaphragm 3) and one

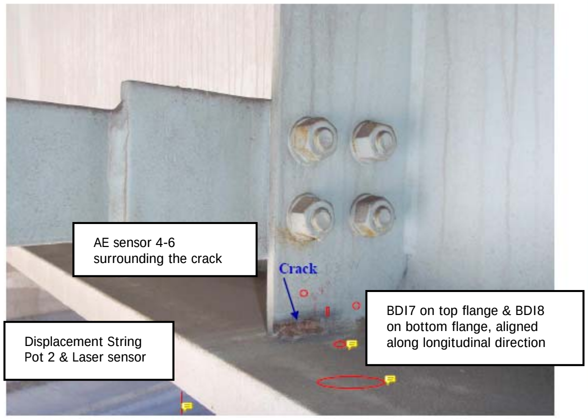

Figure 6. Crack at G4B3D3 (Girder 4 Bay 3 Diaphragm 3) and sensor locations

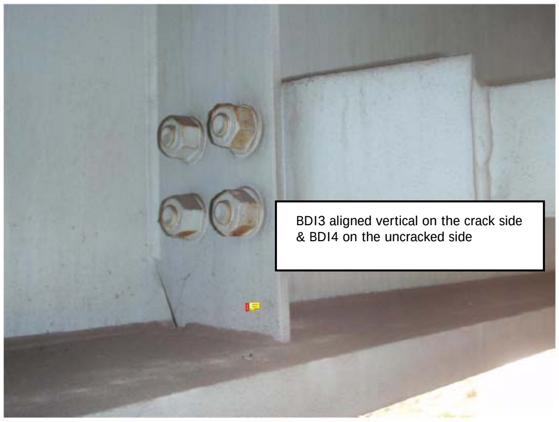

Figure 7. No Sign of Cracking at G4B4D3 (Girder 3 Bay 4 Diaphragm 3) and one sensor

PHASE II – FIELD TEST AND RESULTS

1. <u>Acoustic Emission Monitoring</u>

A total of seven AE sensors were installed on Girder 3 and Girder 4. Three piezoelectric paint AE sensors were installed on Girder 4. Two of the piezoelectric paint AE sensors were placed on the tension side connection plate of Girder 4 where fatigue crack was recently found (see Figure 8) while the third piezoelectric paint AE sensor was placed on the compression side connection plate of Girder 4 to provide ambient noise AE data since there is no active fatigue crack (Figure 9). Figure 10 shows the installation of those AE sensors. Same arrangement is for Girder 3.

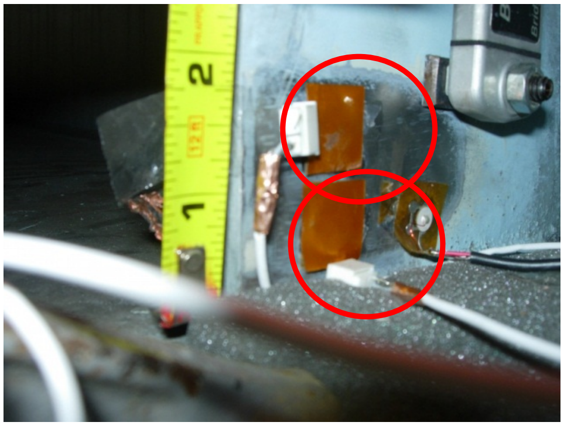

Figure 8. Piezoelectric paint AE sensor on the tension side connection plate (red circled, for monitoring fatigue crack on the weldments between the connection plate and lower flange)

Figure 9. Piezoelectric paint AE sensor (blue circled, for monitoring ambient noise since there is no fatigue crack on this side connection plate)

(a) (b)

Figure 10. (a) Installing AE sensors and wiring; (b) AE data acquisition

Installing AE sensors and wiring took quite some time on March 20 and 21, 2012. The first day (March 19) of field test was spent on surface preparation for installing AE sensors and preparing additional preamplifiers for AE sensors. The second day (March 20) was on installing AE sensors and connecting wires and preamplifier for three AE sensors. During the third day (March 21), most of the time was spent on wire connection and debugging the sensors. Data were collected from all seven AE sensors. Continuous AE monitoring was carried out from approximately 1:10pm to 1:55pm on March 21, 2012. Trigger threshold was set to be 50 mV for each AE sensor channel over this monitoring period, that is, if the AE signal for each chancel exceeds 50 mV, data collection would be triggered and a total of 10,000 data points (5 msec.) will be collected for each channel at a sampling rate of 2 MHz. Over this monitoring period, no fatigue-crack-related AE signal is observed. Samples of AE data and their frequency characteristics (by applying FFT on time series data) are shown in Figure 11. This is probably due to the short AE monitoring period (only 45 minutes) during this field test and as such possible AE activities due to fatigue crack growth might be missed. It is recommended in the next field test, a longer monitoring period (e.g., at least three days) will be arranged to collect AE signals related to fatigue crack growth.

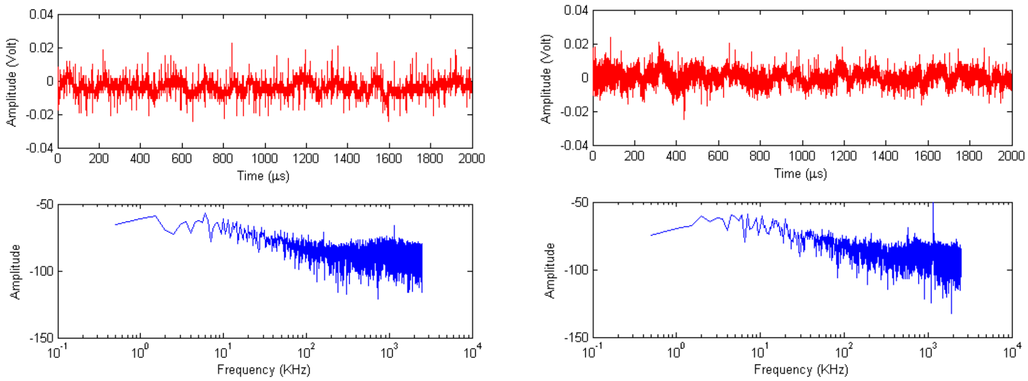

(a) Data from Ch3, piezo paint AE sensor (b) Data from Ch4, piezo paint AE sensor

Figure 11. AE data collected by piezo paint AE sensor on Girder 4: (a) on tension side connection plate with existing fatigue crack; (b) on compression side connection plate without crack

2. <u>Wireless Sensor (monitoring vibration responses of Girders 2 to 5 of the bridge)</u>

A total of four wireless accelerometers (see Figure 12) Imote2 were used to monitor the vibration responses of the bridge. One wireless sensor was installed on one of the girders (Girder 2 to 5) and acceleration data was acquired at 100 Hz sampling rate synchronically. The acceleration data was used to provide modal frequency information (Figure 13) that can be used to calibrate the finite element model of the bridge. The fundamental frequency thus measured is 3.22 Hz, which is very close to the value from finite element analysis (3.14 Hz).

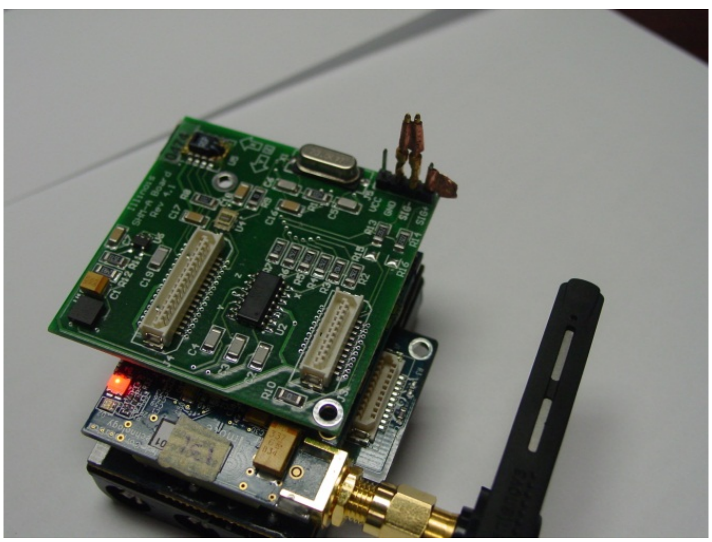

Figure 12. Wireless sensor Imote2 (measuring acceleration and temperature)

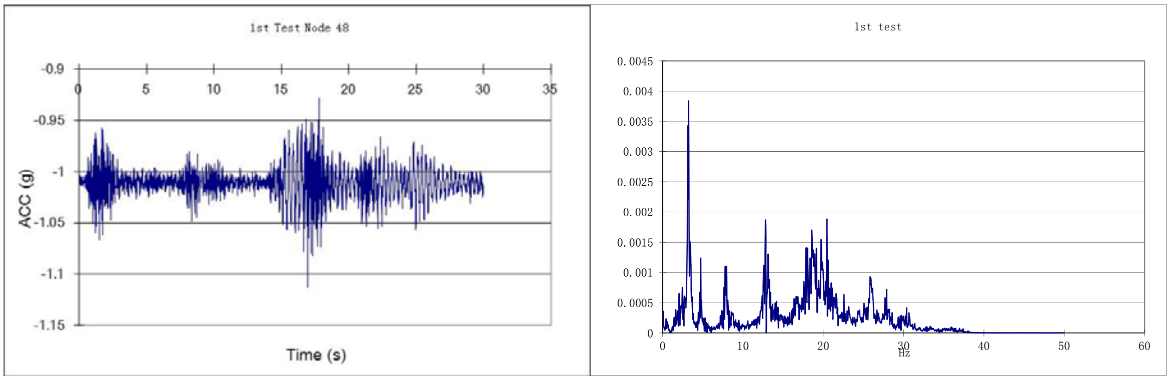

(a) Acceleration time history

(b) FFT of acceleration data (horizontal axis: frequency; vertical axis: FFT amplitude)

Figure 13. Acceleration data measured by wireless sensor

3. Bridge Deflection Monitoring

Both laser sensor and ultrasonic distance sensors were used to measure the dynamic deflection of the bridge, as shown in Figure 14. Only one laser sensor and one ultrasonic distance sensor were used each time. The data from laser sensor is shown in Figure 15. The measured deflection value from the laser sensor agrees well with the string pot, and its accuracy is also validated by the fundamental frequency indicated by FFT of the laser sensor measured deflection data (see Figure 16). The ultrasonic sensor data had some problems, most likely due to a high sampling rate (20 Hz seems to be too high for ultrasonic distance sensor of this particular model, next time we will lower the sampling rate to 5 Hz, which provides much better accuracy during lab calibration test) and parasitic echo signals from reflecting background such as lower surface of bridge deck (next field test we will install the ultrasonic distance sensor on the girder and let it shoot down on road surface to avoid background noise).

Table 1. Maximum deflection measured by laser sensor

Girder #	3	4	5
MaxD (m)	0.0066	0.0069	0.0063

Note: MaxD=average(Disp)-minimum(Disp)

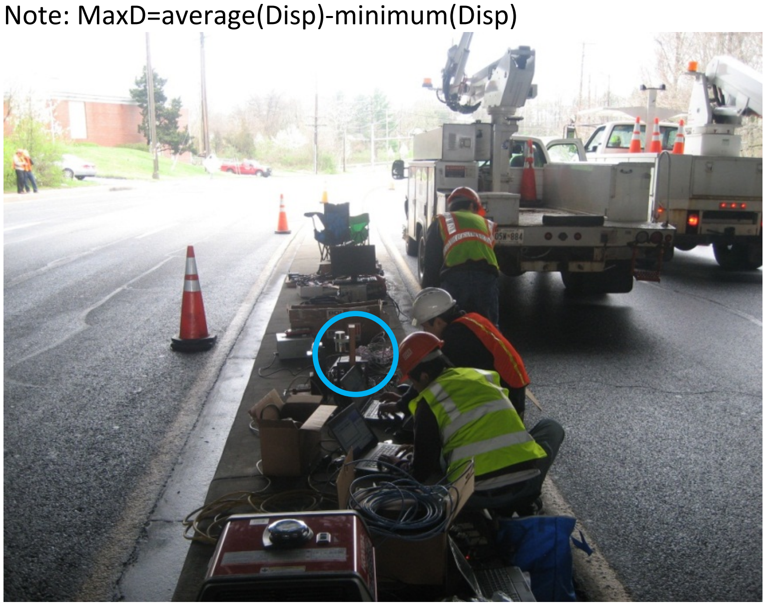

Figure 14. Bridge deflection measurement with ultrasonic distance sensor and laser distance sensor (in blue circle)

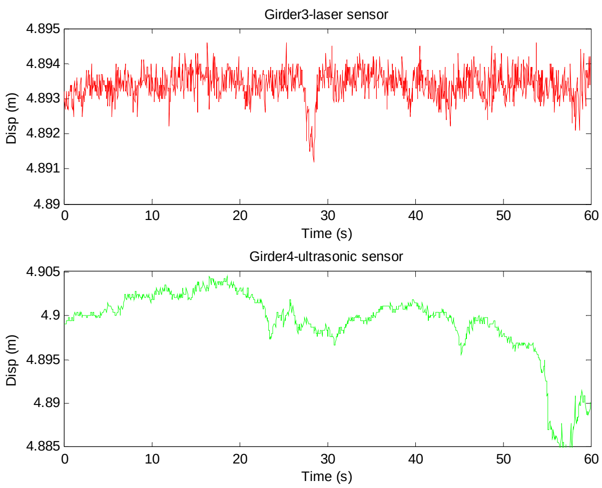

Figure 15. Bridge deflection data by laser sensor (upper) and ultrasonic sensor (lower)
(The measured value is the distance between the sensor and girder bottom surface)

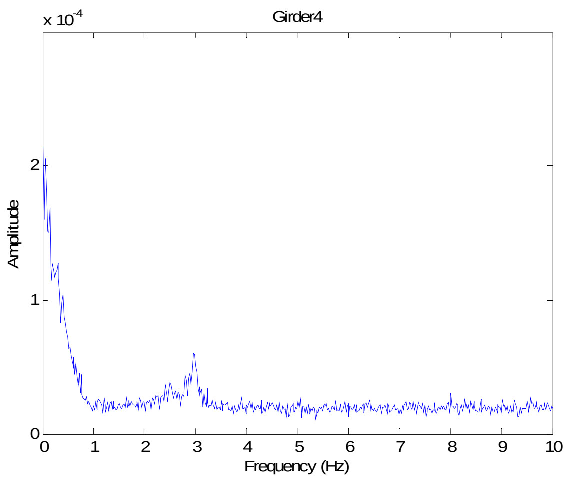

Figure 16. FFT of laser distance sensor
(note the existence of fundamental frequency of the bridge near 3 Hz)

4. <u>BDI Strain Transducers</u>

BDI 1-4 strain transducers were placed on both sides of the connection plates while BDI 5- 8 were placed on the top and bottom flanges on Girders 3 and 4 (Figures 4-7). Since each transducer is unique and individually calibrated, their numbers are marked on Figure 17 for identification. Figures 18 and 19 are showing the stresses on the flanges and connection plates, respectively.

The maximum stress measured on the bottom flange is 1.604 ksi in tension for BDI 3215 on the bottom flange of girder 3. As for the connection plates, the maximum stresses are are 16.18 ksi in tension for BDI 1641 on girder 3 and 16.1 ksi in tension for BDI 1644 on girder 4.

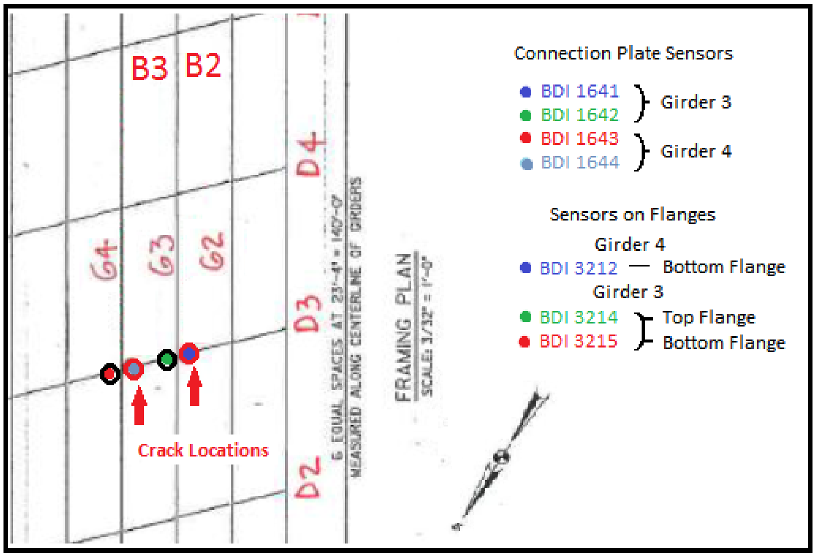

Figure 17. BDI strain transducer locations and marked numbers

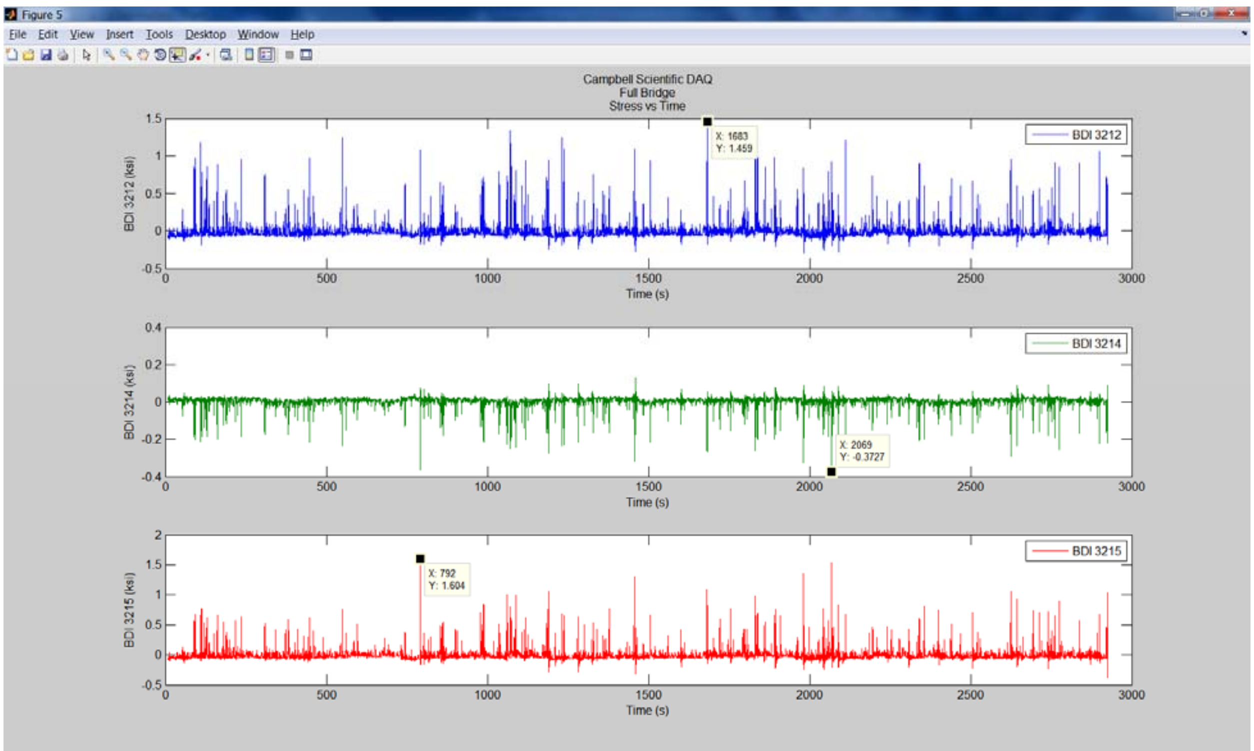

Figure 18. BDI strain transducer flange measurements on girders 3 and 4
(Positive indicates compression; 3212 G4 top flange; 3214 G3 top flange and 3215 G3 bottom flange)

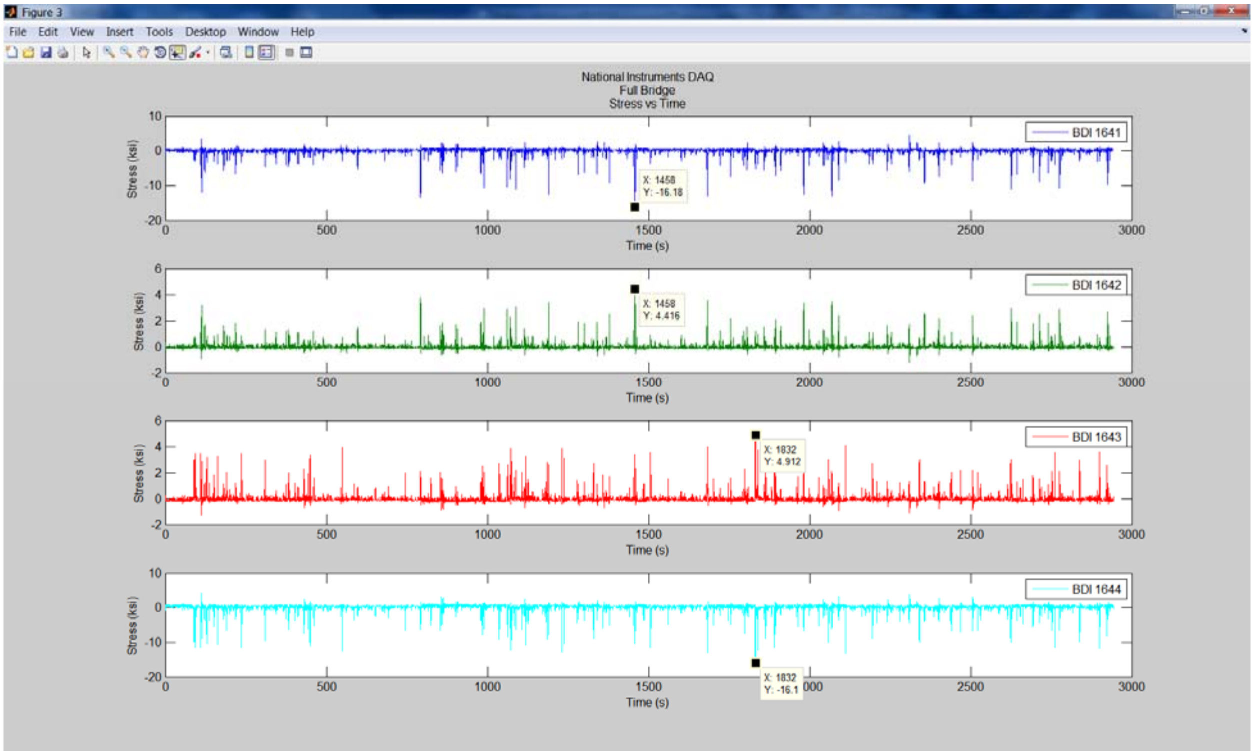

Figure 19. BDI strain transducer connection plate measurements
(Positive indicates compression; 1641 G3 crack side; 1642 G3 uncrack side, 1643 G4 crack side and 1644 G4 uncrack side)

5. <u>String Pots</u>

String pots were placed on girders 3 and 4, synchronized with strain and acoustic emission results. The maximum measurements within the testing period are 0.231” on girder 3 and 0.205” on girder 4, respectively, which are very closed to the laser results, though laser was independently measured. (This short-term measurement is lower than previously measure up to 0.5” or 0.75”.)

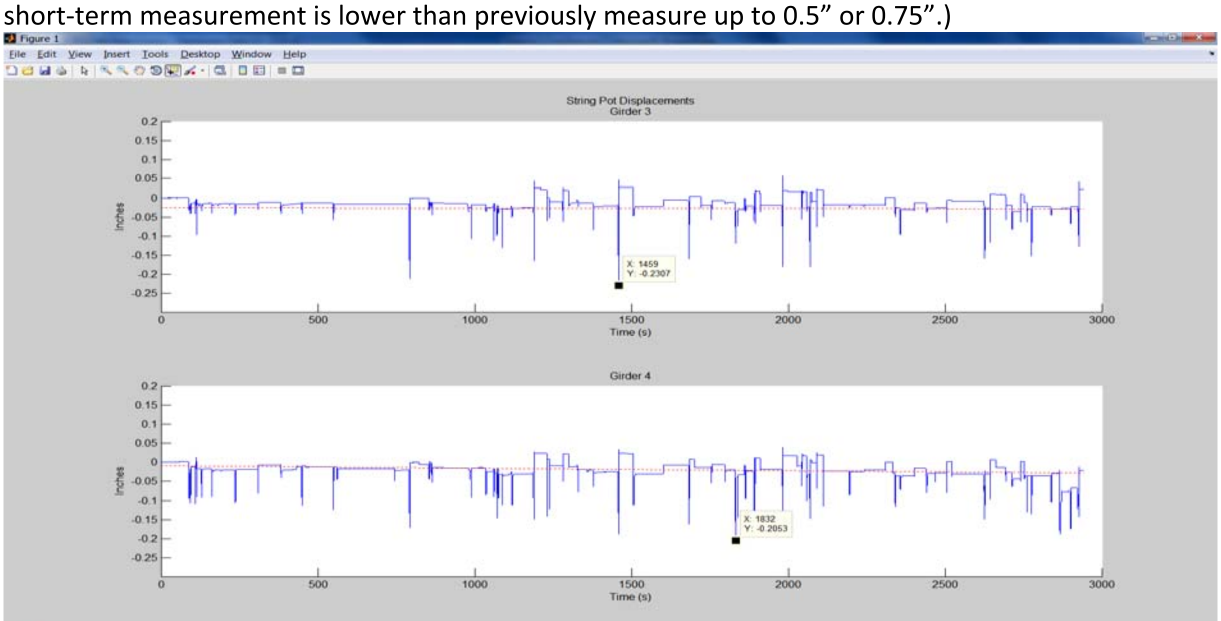

Figure 20. String pot deflection results on girders 3 and 4

PHASE III – FEM ANALYSIS

Finite element model was generated for the bridge. Its model is shown in Figure 21 and its first natural frequency is around 3.11 for a fixed-fixed boundary condition and lower for the normal analysis of fixed-free boundary condition. For comparing the first mode, fixed-fixed condition is more realistic where the test result is 3.22 Hz and FEM result for fixed-fixed condition is 3.14 Hz (Table 2).

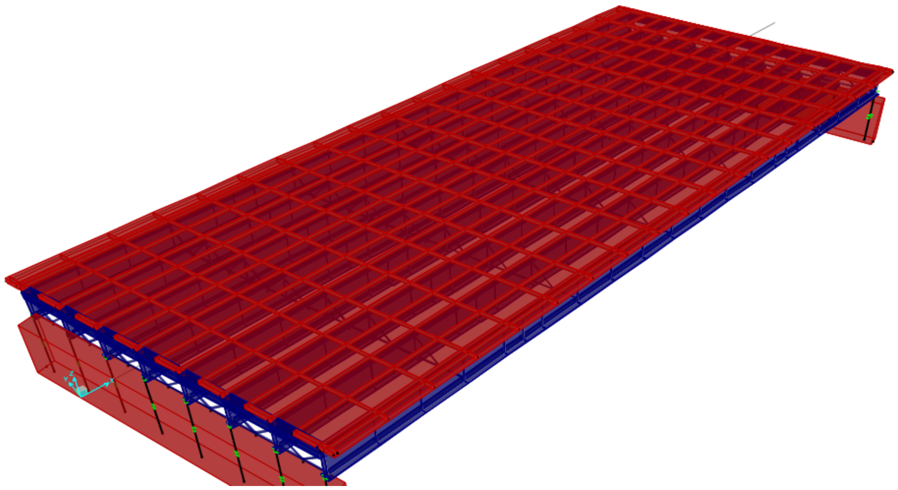

Figure 21. FEM model of the Middlebrook Road Southbound Bridge by CSI Bridge

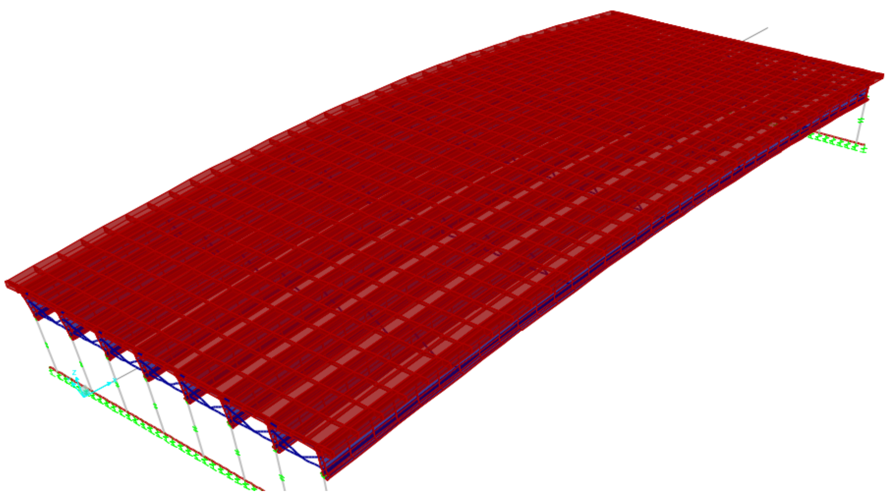

Figure 22. Modal shape of the first mode (f = 3.136 Hz) by CSI Bridge

Table 2 – Natural frequencies by FEM analysis

Hz	Fixed-Fixed	Fixed-Free
1	3.136131	2.235395
2	3.204958	2.730252
3	5.483081	5.030165
4	5.581643	5.16084
5	6.518478	6.48045

To simulate the traffic, Weigh-in-Motion data was collected from the Hyattstown southbound station, which is located on I270 about 10 miles north of the tested bridge. The more accurate simulation process is still under development. In order to get approximate traffic loading, seven cases of HS-20 truck loading with run stream on different lanes of different patterns were simulated which are:

Case 1: 3 trucks passed the bridge one by one

Case 2: the 3rd truck entered the bridge when the 1st truck just left the bridge (only two trucks on the bridge at the same time)

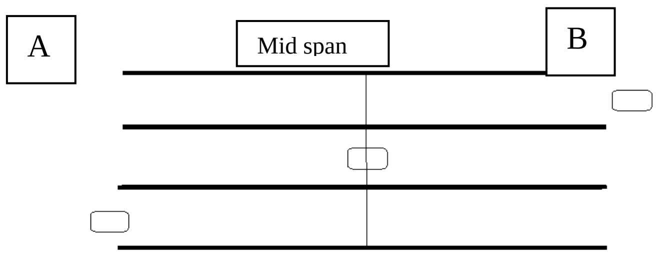

Case 3: the 3rd truck entered the bridge when the 1st truck and 2nd truck just left mid span

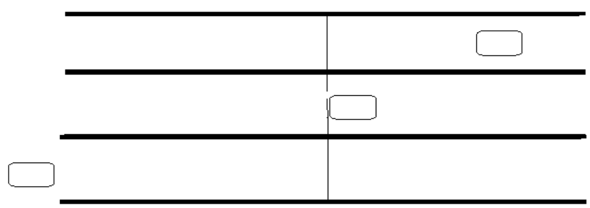

Case 4: the 1st truck left the bridge when the 2nd truck and 3rd truck just entered the right span one after the other

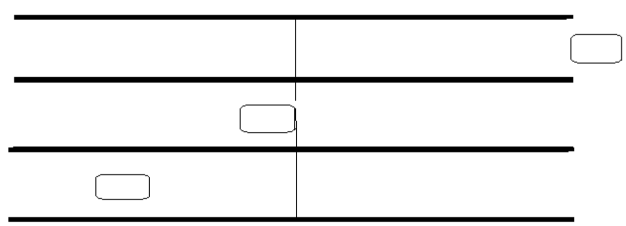

Case 5: the 1st truck and the 2nd truck passed the bridge parallel

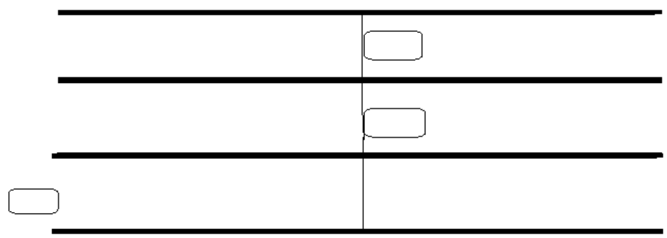

Case 6: the 1st truck just left when the 2nd & 3rd truck is @ mid span

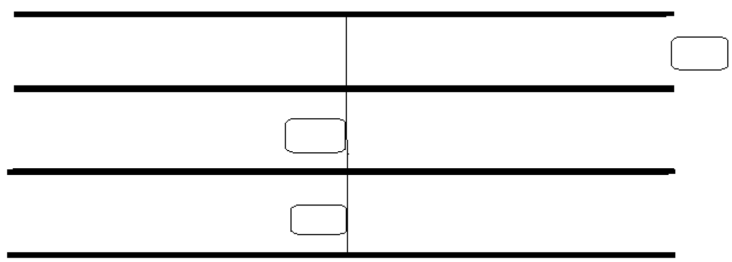

Case 7: 3 trucks passed the bridge at the same time, no truck load reduction is applied

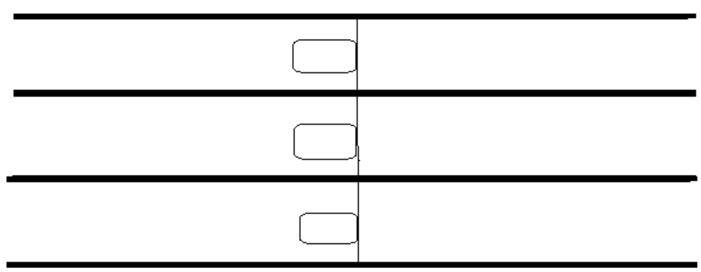

Table 3 – Maximum bottom flange stress ranges and deflections of seven truck simulation cases

	GIRDER3	GIRDER4	GIRDER3	GIRDER4
LL_CASE	stress(ksi)	stress(ksi)	defl (in)	defl (in)
CASE1	1.229	1.281	-0.219	-0.189
CASE2	1.249	1.343	-0.250	-0.224
CASE3	1.239	1.281	-0.223	-0.188
CASE4	1.507	1.486	-0.220	-0.277
CASE5	1.189	1.316	-0.263	-0.317
CASE6	1.926	2.128	-0.366	-0.355
CASE7	2.245	2.369	-0.435	-0.471

Since this is a simple-span bridge, the maximum stress ranges at the bottom flange are close to the maximum stresses, which are demonstrated in Figure 18. The maximum stress measured on the bottom flange of girder 3 is 1.604 ksi where the FEM maximum stress ranges for case 4 for two HS-20 loaded subsequently on two near lanes is 1.507 ksi and case 6 for two HS-20 loaded on two near lanes is 1.926 ksi, respectively. Case 7 for three lane lsimultaneously oaded, based on AASHTO LRFD Specifications that can be reduced by a multiple presence factor of 0.85, yields 1.908 ksi (0.85*2.245 ksi). Global tress contour and its close-up view (in kips/ft^2; divided by 144 to convert the scale to ksi) are shown in Figure 23 (a) and (b). Maximum girder deflections are also shown on the same table for reference. Due to program limitation, the connection plates were not modeled.

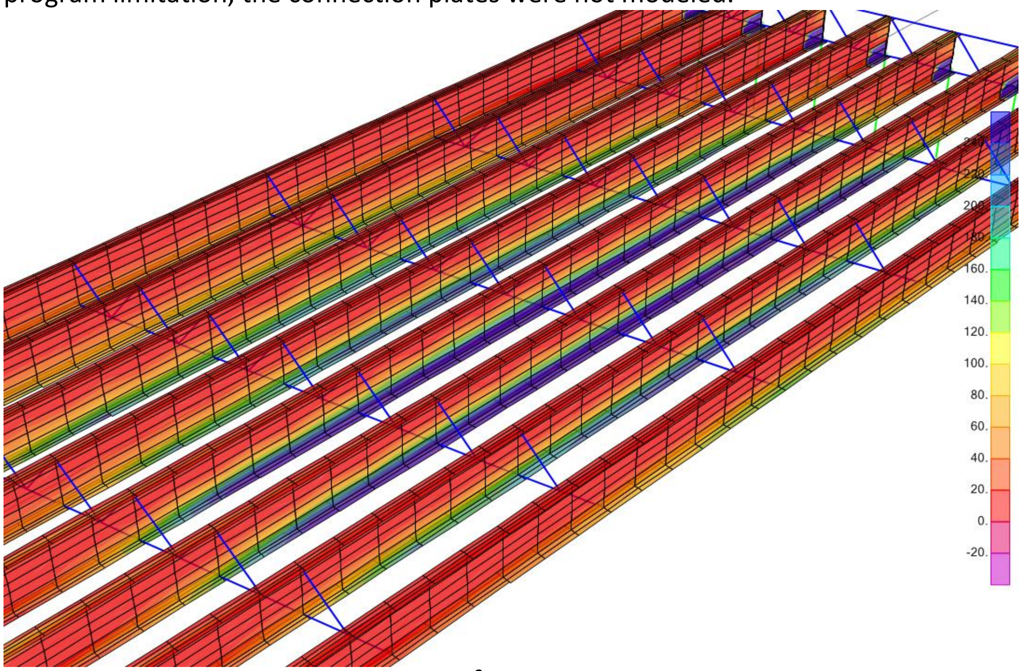

(a) Global stress contour (in kips/ft^2) of eight southbound girders (looking south)

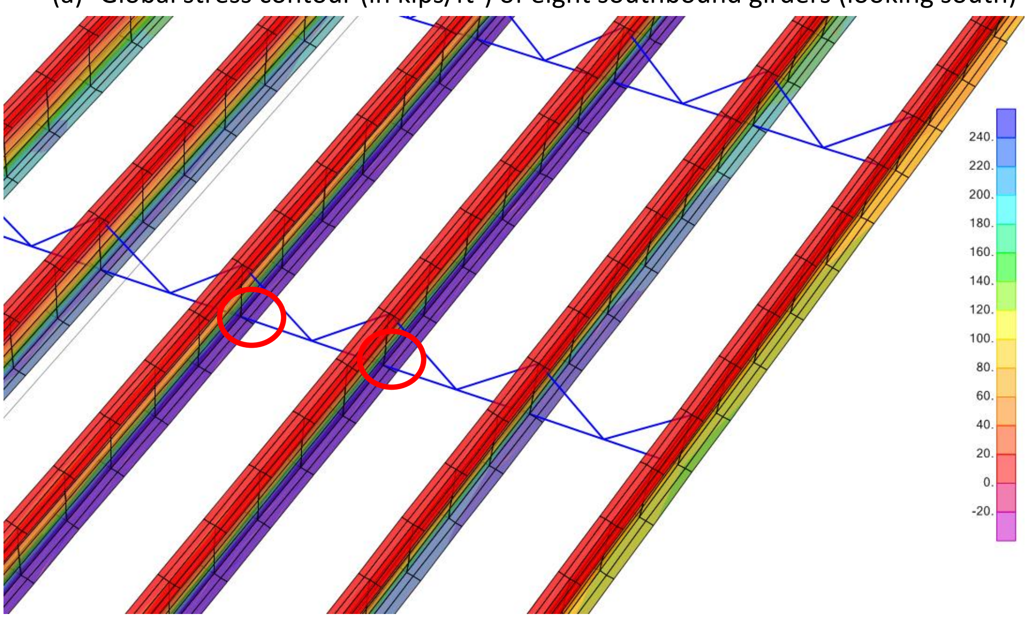

(b) Close-up view of girders 3 and 4 with fatigue cracks

Figure 23. Live load stress contour of truck loading case 6

<u>High tension stress on the connection plates on girders 3 and 4</u>

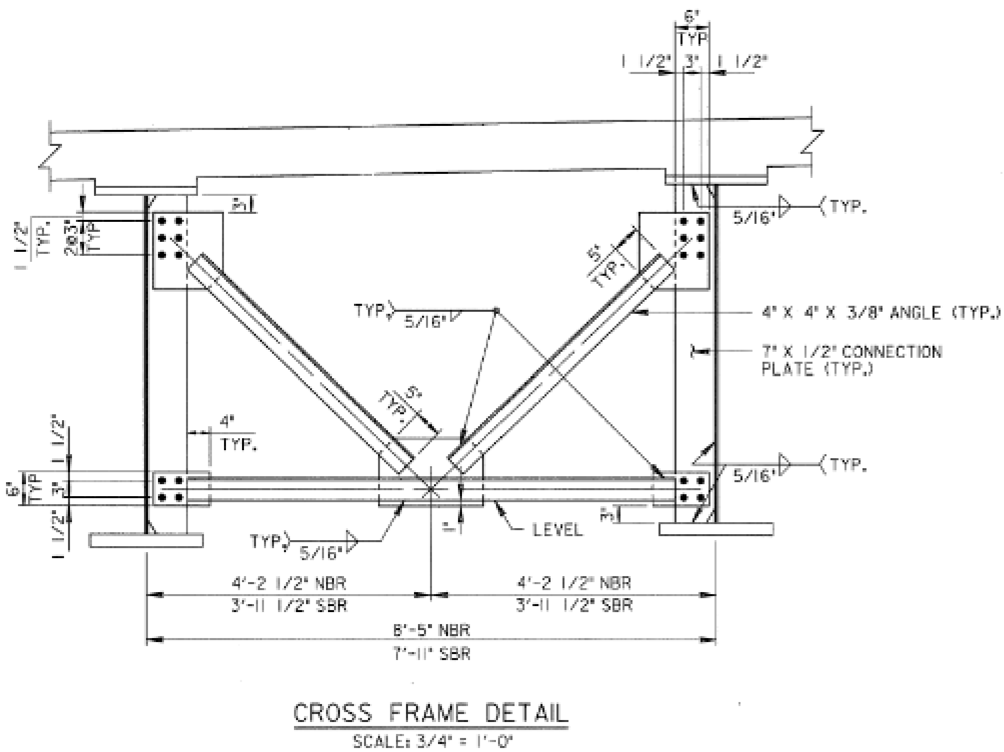

Figure 24. Typical cross frame detail

Out of all types of cross-frames, X-type with top and bottom chords is the stiffest of all, then the K-type with top and bottom chords, then the X-type with bottom only and the flexible one is the K-type with bottom chord only. Differential displacement between girders will cause one diagonal in tension and one in compression. Since the working point of the diagonal is not at the junction of girder web and top flange plus no help from the top chord, one side of the connection plate will be under tension and one under compression. Measured 16.1 ksi in tension is not surprising with the flexibility of the cross-frame and the girder system (with up to 0.5” to 0.75” vertical deflections due to live load observed.)

Appendix C - NCST Report for NC Structure No. 060025 Swing Bridge at Beaufort County

1-TECHNICAL STATUS

Accomplishments by milestone

- Analyzed and organized detailed structural information of the Swing Bridge at Beaufort County

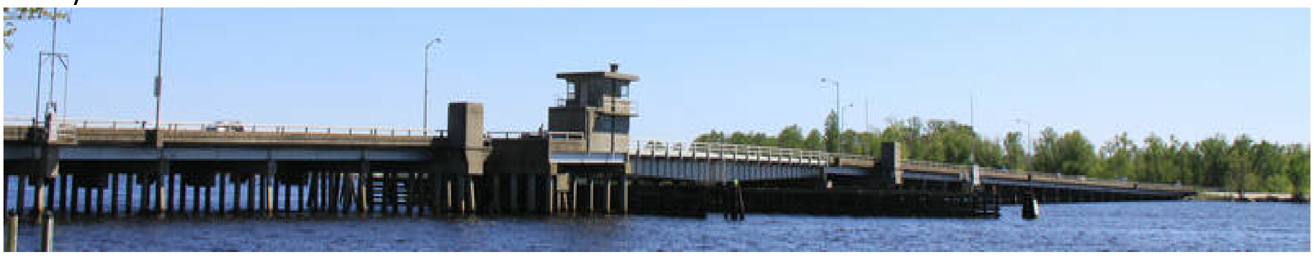

Figure 1 Full scope of the bridge

It can be seen from Figure 1 that the bridge consists of side span and main span, the structural support of the side span is a simply supported girder bridge, which there is no need to be monitored because of its simple stress state. The boundary condition of the main span can change from a simply supported girder bridge to a cantilever girder bridge when the main span is close or open. Considering the complex stress state, the main span will be subjected to be monitored for the dynamic behavior of the bridge. Figure 2 shows the details of the main span.

Figure.2 Boundary supports of the main span

We can infer the dynamic behavior from its mode of vibration, which can be obtained by a few of accelerometers. Figure 3 the theoretical first and second mode shapes for simple supported structure and cantilever structure. Assume the entire length of the beam is L. Accelerometers need to be installed at the characteristic locations of those two mode shapes, that is, x=0, 1/4L, 3/8L, 1/2L, 5/8L, 3/4L, L. The locations of sensors are shown in Figure 4. There are needed at least 7 sensors in this system to monitor the dynamic behavior of the bridge.

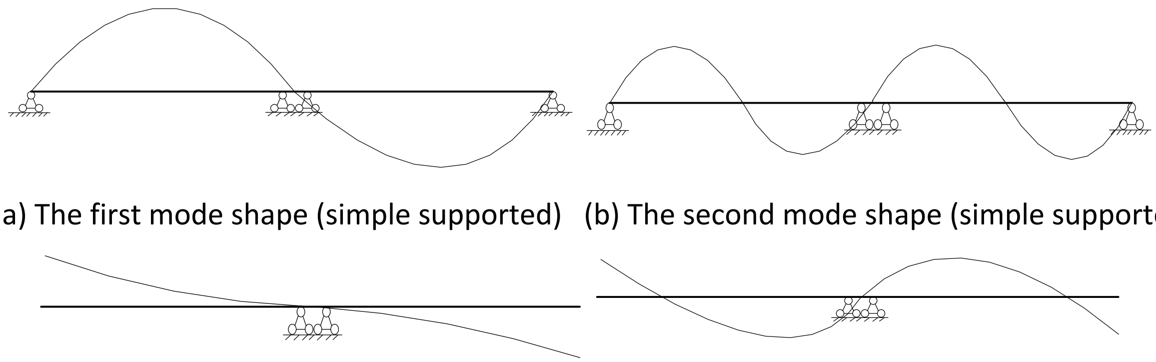

(a) The first mode shape (simple supported) (b) The second mode shape (simple supported)

(a) The first mode shape (cantilever) (b) The second mode shape (cantilever)

Figure 3 Various vibration modes

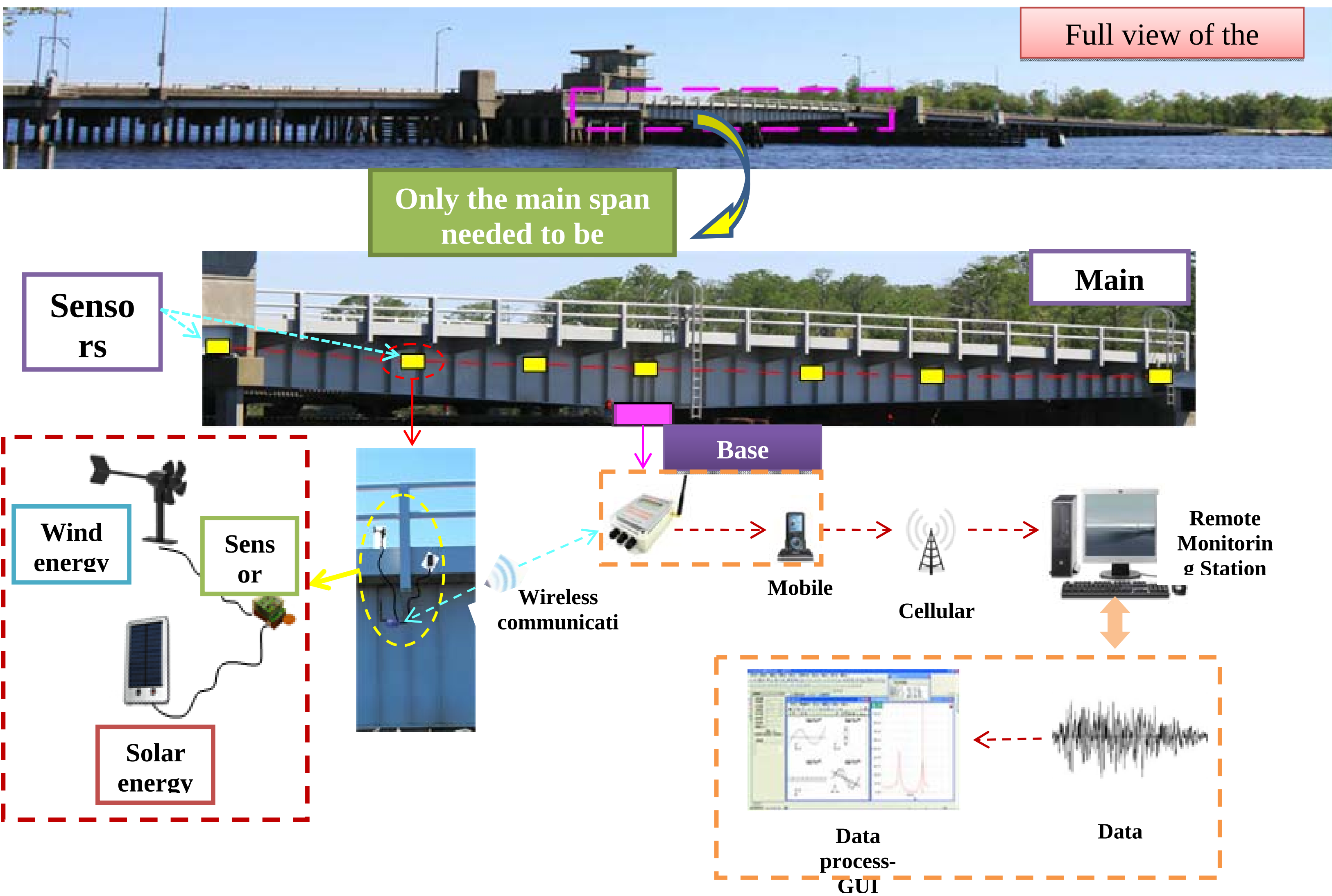

Figure 4 Sketch plan for monitor system

- Developing signal and data transmission paths (Gateway Protocol)
  The sensors collect the raw data of the bridge from each wireless sensor and send it to the base station in the form of signal, then save or upload the data to the remote console. Therefore we should create a program to realize the function that the base station can receive the signal sent from sensors by serial port, that is the first step, and then we should save or send the data signal directly to remote console. Figure 5 is the visualized data transmitting software interface.

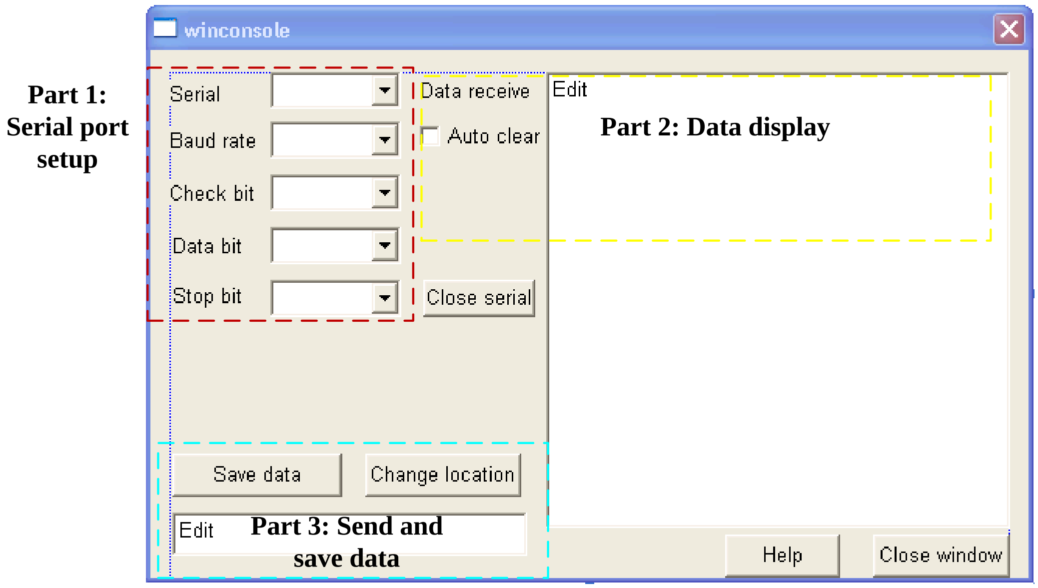

Figure 5 The visualized data transmitting software interface

- Designing and manufacturing wind turbine energy harvester-based on the experimental result of the miniature wind turbine (MWT), which can be used to collect wind energy in the field has been designed and manufactured(Figure 6).

Figure 6 The miniature wind turbine

- Developing and evaluating a new Buck-Boost Converter (Figure 7)-A new Buck-Boost Converter has been designed for storing the energy extracted from the wind energy. The values of various elements in this boost converter also have been initially determined. The next task is manufacturing the Buck-Boost Converter and verifying the effectiveness of the Buck-Boost Converter.

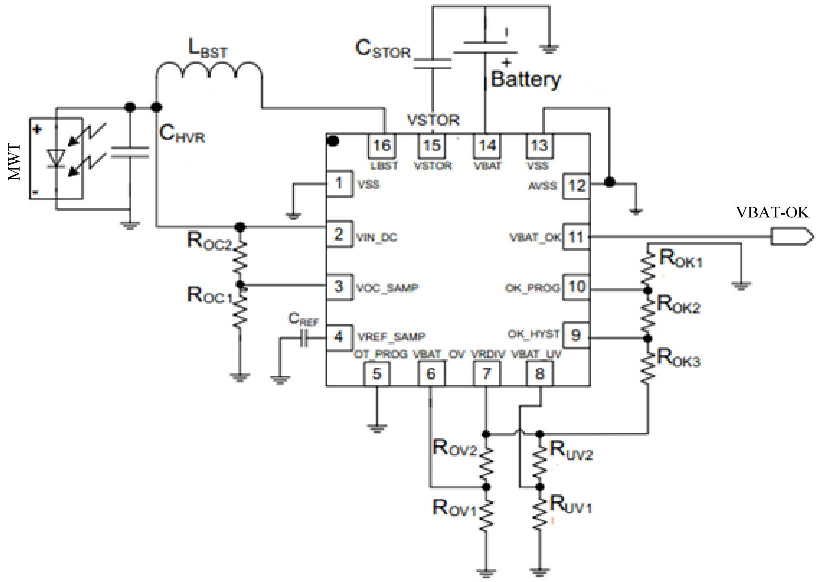

Figure 7 The Buck-Boost Converter

- Developed a new wireless accelerometer board. The new wireless accelerometer board uses an ultra low-power high performance three axes linear accelerometer: LIS331DLH (Figure 8). It has dynamically user selectable full scales of ±2g/±4g/±8g and it is capable of measuring accelerations with output data rates from 0.5 Hz to 1 kHz.

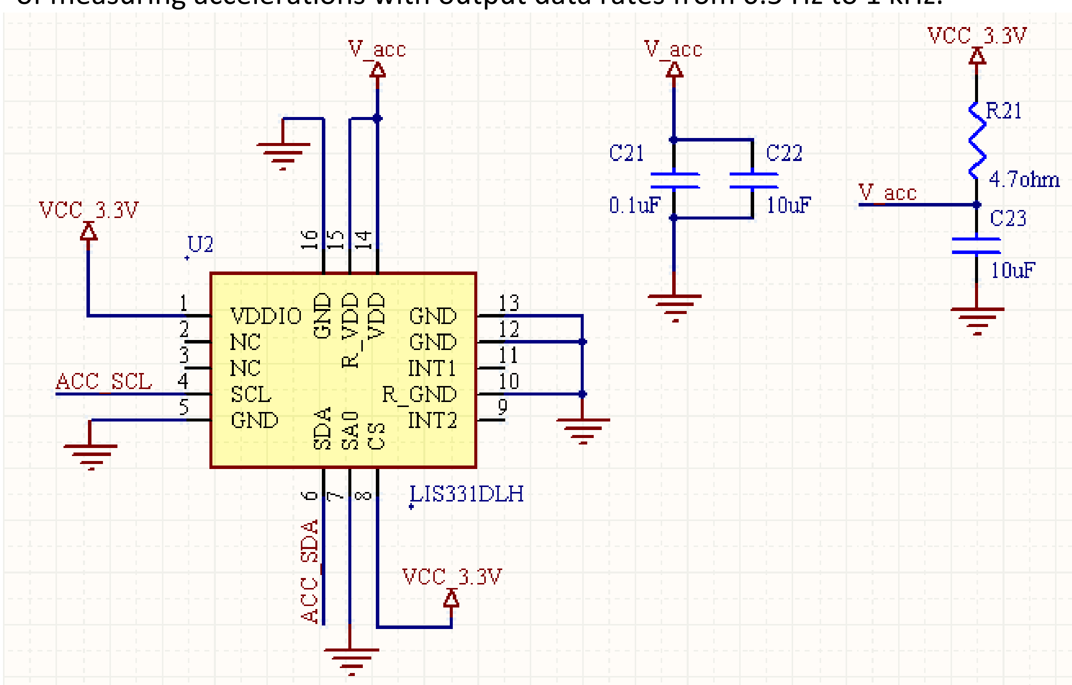

Figure 8 The Schematic of LIS331DLH

The new wireless accelerometer board uses a 32 Mbit SPI Serial Flash chip-SST25VF032B (Figure 9) to store the acceleration data. The SST25VF032B device has a four-wire, SPI-compatible interface and is enhanced with improved operating frequency which lowers power consumption.

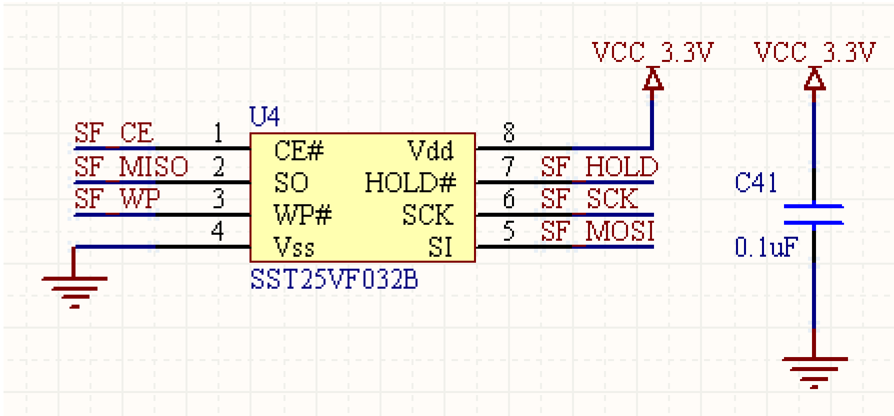

Figure 9 The Schematic of LIS331DLH

- This board also has a solar energy charge circuit for a Li-Ion battery. The charger circuit uses LTC1734 (Figure 10). It's a low cost, single cell, constant-current/constant-voltage Li-Ion battery charger controller. Charge current can be monitored via the voltage on the PROG pin allowing a microcontroller to read the current and determine when to terminate the charge cycle.

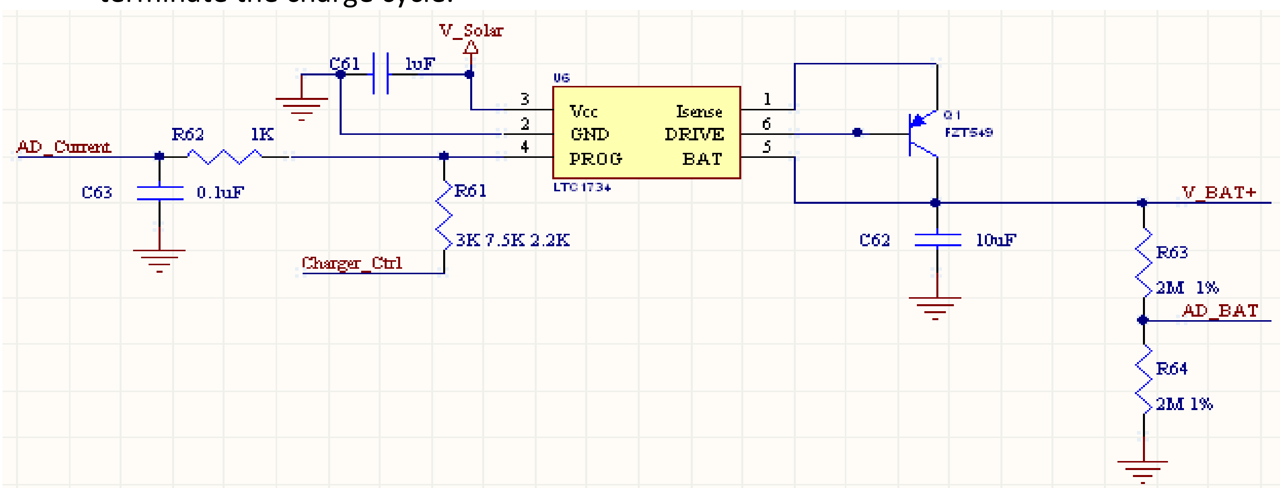

Figure 10 The Schematic of LTC1734

Future plan:

- Finishing the signal and data transmission programs before the accelerometers installed.
- Manufacturing the Buck-Boost Converter. The miniature wind turbine system to be capable of converting wind energy into electrical energy and storing it in rechargeable battery will be finished.
- Finish the PCB design of the new wireless accelerometer board and send the design to PCB factory, write programs to debug it.
- Order the circuit components and solder the new wireless accelerometer boards and solar energy panel and Lithium battery.
- Assemble the wireless accelerometer sensors